

*Full Paper*

## **Aluminum Corrosion Inhibition by 2,6-diaminopyridine in 3.5% NaCl: Tafel Polarization, Surface and Quantum Chemical Study**

**Kashif R. Ansari\* and Mumtaz A. Quraishi**

*Department of Chemistry, Indian Institute of Technology (Banaras Hindu University),  
Varanasi -221005, India*

\* Corresponding Author, Tel.: +91-8896562533

E-Mail: [kansari.rs.apc13@itbhu.ac.in](mailto:kansari.rs.apc13@itbhu.ac.in), [ka3787@gmail.com](mailto:ka3787@gmail.com)

*Received: 13 October 2015 / Received in revised form: 8 February 2016 /*

*Accepted: 9 February 2016 / Published online: 31 March 2016*

---

**Abstract-** The inhibition property of 2,6-diaminopyridine for aluminum in 3.5% NaCl was carried out by using Tafel polarization, Scanning electron microscopy (SEM), Atomic force microscopy (AFM) and quantum chemical methods. Tafel polarization study reveals that inhibitor is of mixed type but predominantly anodic. The maximum inhibition is 98.5% at 100 mg/L. Surface analysis (SEM and AFM) supports the formation of a protective inhibitor film on the aluminum surface. Quantum chemical calculation has performed for both neutral and protonated molecules in order to study the effect of molecular structure on inhibition efficiency.

**Keywords-** Aluminum alloy, Tafel polarization, SEM, AFM

---

### **1. INTRODUCTION**

Aluminum and their alloys are commonly used in the transport applications, aviation industry, bicycle components, hang glider airframes [1–5] due to their high strength-to-density ratio. Aluminum is naturally protected from corrosion due the formation of oxide

layer over its surface, but it may corrode when exposed to aggressive environments. Especially in presence of seawater this oxide layer breaks down due to the presence of chloride ions ( $\text{Cl}^{-1}$ ).

Most common way to cease the corrosion process is use of inhibitors because it doesn't require any special equipment, its low-cost and easy operation. In literature many corrosion inhibitors have been used but most of them are toxic either towards the environmental or health. So, it becomes very much essential to used eco-friendly inhibitors for Al.

In present study we have studied the corrosion inhibition effect of 2, 6-diaminopyridine on aluminum by using Tafel polarization. Meanwhile aluminum surface was analyzed AFM and SEM techniques. To support the experimental results quantum chemical study was carried out both on neutral and protonated molecule.

## 2. EXPERIMENTAL WORK

### 2.1. Materials and solutions

Aluminum alloy used has following composition (wt.%): Si=0.77, Fe=0.93, Cu=0.02, Mn=0.11, Mg=0.01, Zn=0.01, Cr=0.05, Ti=0.02, V=0.01, Ga=0.01 and balance Al. The dimension of aluminum strip used for potentiodynamic polarization test is 30.0 mm×3.0 mm×3.0 mm. Aluminum alloy was polished with emery papers of 600-1200 grades, degreased with acetone, and dried before experiments. The test solution i.e. 3.5% NaCl was prepared by analytical grade NaCl with double distilled water and all experiments were carried out in unstirred solutions at 308 K.

### 2.2. Inhibitor

2, 6-diaminopyridine was purchased from Sigma-Aldrich and its molecular structure is given in Fig. 1.

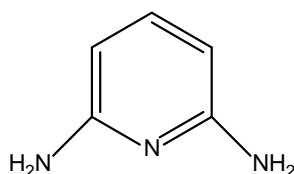


**Fig. 1.** Molecular structures of inhibitor

### 2.3. Electrochemical measurements

For electrochemical study a three electrode cell assembly was used, where aluminum strip acts as a working, platinum as counter and saturated calomel as reference electrodes were used respectively. All electrochemical experiments were conducted at 308 K temperature by using Gamry Potentiostat /Galvanostat (Model G-300). For data analysis Echem Analyst 5.0 software package was used.

Tafel polarization measurements were performed by changing the electrode potential automatically from -0.25 to +1.00 V versus SCE at OCP at a scan rate of 1 mVs<sup>-1</sup>. All experiments were done after immersion for 60 min in 3.5% NaCl in the absence and presence of inhibitor.

## 2.4. Surface morphology

Surface analysis was carried out by using SEM and AFM. In both SEM and AFM study aluminum specimens were exposed to 3.5% NaCl solution in the absence and presence of optimum concentration (100 mg/L) of inhibitor for 24 h in temperature range of 308-328 K. The SEM was performed by a Ziess SUPRA 40 instrument model, with magnification of 5 kx. The instrument used for AFM is (NT-MDT SOLVER Next AFM/STM). The scan size of each sample is 5.0 μm × 5.0 μm.

## 2.5. Quantum chemical study

The optimization of inhibitor molecule was done by using B3LYP Density Functional Theory formalism (DFT) with 6-31 G (d, p) basis set, using Gaussian-03 [6]. Quantum chemical parameters studied are Energy of the Highest Occupied Molecular Orbital ( $E_{HOMO}$ ), Energy of the Lowest Unoccupied Molecular Orbital ( $E_{LUMO}$ ) and Energy gap between HOMO and LUMO ( $\Delta E$ ).

## 3. RESULTS AND DISCUSSION

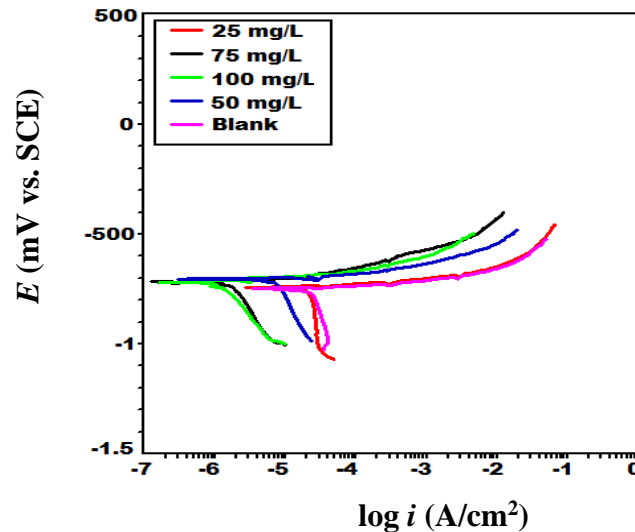
### 3.1. Tafel polarization

Fig. 2 shows the polarization curves for aluminum in 3.5% NaCl solutions in absence and presence of different concentration of inhibitor. The  $I_{corr}$  values were calculated from the cathodic branch of polarization curve [7,8].

**Table 1.** Tafel polarization data for aluminum alloy in 3.5% NaCl for different concentration of inhibitor

Inhibitor	Conc. mg/L	$E_{corr}$ (mV/SCE)	$I_{corr}$ (μA/cm <sup>2</sup> )	$\beta_a$ (mV/dec)	$-\beta_c$ (mV/dec)	$\eta$ (%)
Blank	--	-746.7	55.06	29.73	3063	--
Inhibitor	25	-741.3	36.77	28.62	2390	33.21
	50	-703.4	14.19	28.16	634.7	74.22
	75	-713.7	10.31	29.87	504.0	81.27
	100	-718.1	0.80	22.88	379.8	98.54

All electrochemical parameters like corrosion potential ( $E_{\text{corr}}$ ), Corrosion current density ( $I_{\text{corr}}$ ), cathodic Tafel slope ( $\beta_c$ ) and anodic Tafel slope ( $\beta_a$ ) were calculated and summarized in Table 1.



**Fig. 2.** Tafel polarization plots for aluminum alloy in 3.5% NaCl

The  $\eta\%$  values were calculated by using the following equation [9-14]:

$$\eta\% = \left(1 - \frac{I_{\text{corr}(i)}}{I_{\text{corr}}}\right) \times 100 \quad (1)$$

It can be easily observed from Table 1 that with the addition of inhibitor, the  $E_{\text{corr}}$  values was shifted towards more active direction i.e. towards anodic side

From the potentiodynamic polarization curves (Fig. 2), it can be observed that anodic branches in absence and presence of inhibitor show an active behavior and on the cathodic branch, a cathodic limiting current can be observed, which is due to the oxygen reduction. As the inhibitor concentration increases, both anodic and cathodic curves were shifted towards the lower current density. This phenomenon implies that the inhibitor is reducing both the anodic and cathodic reactions and act as the mixed type inhibitor [15]. But the  $E_{\text{corr}}$  values are shifting towards the positive direction with respect to blank. So, overall the inhibitor is mixed type but anodically dominant. Also, as the concentration of inhibitor is increased there is decreased in the  $I_{\text{corr}}$  values, due to adsorption of inhibitor [16-22].

## 3.2. Surface morphology

### 3.2.1. SEM

The adsorptive nature of inhibitor over aluminum is established by SEM technique and obtained micrographs at different temperatures are given in Fig. 2 (a-f).

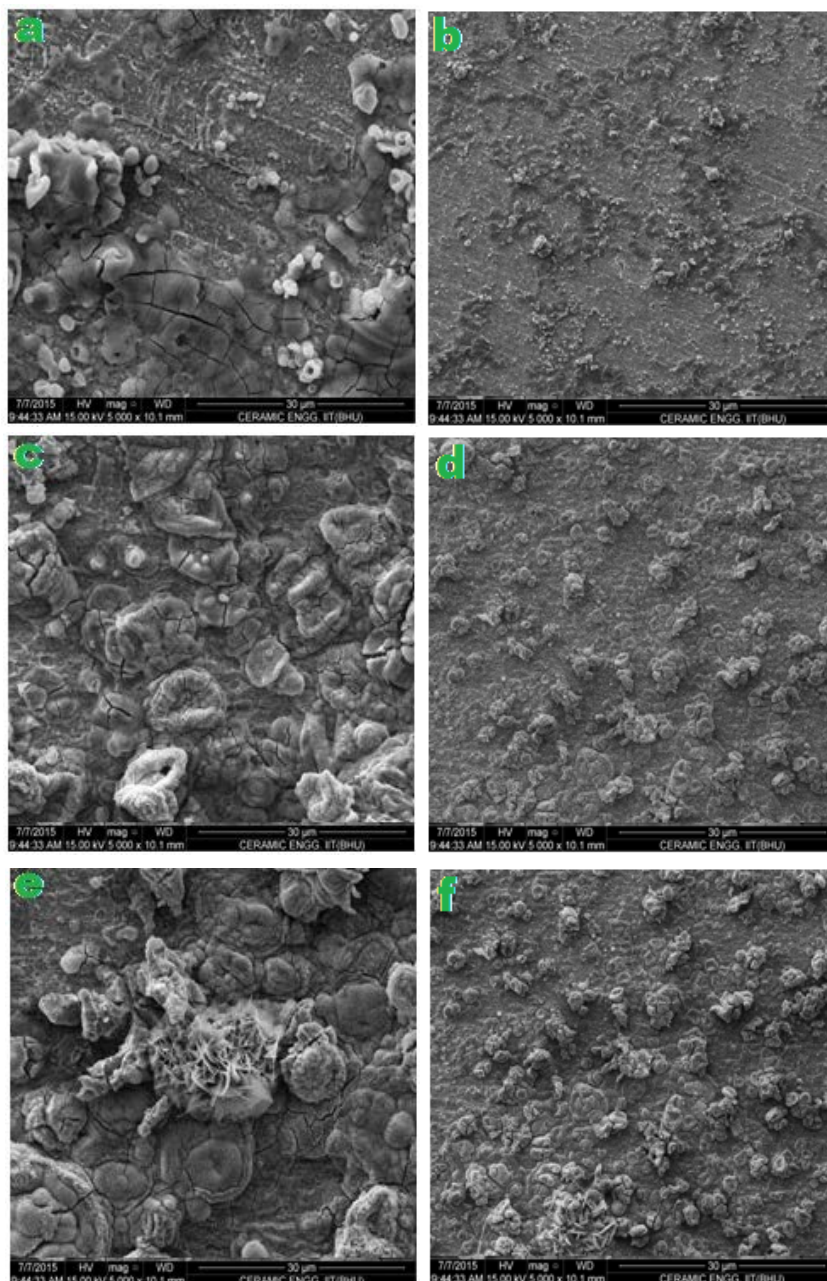


**Fig. 2.** SEM images (a) Blank at 308 K; (c) Blank at 318 K; (e) Blank at 328 K; (b) Inhibitor at 308 K; (d) Inhibitor at 318 K; (f) Inhibitor at 328 K

The morphologies in the blank solution are given in Fig. 2a at 308 K, Fig. 2c at 318 K, Fig. 2e at 328 K. These images reveal the presence of much corroded surface, with pits and cracks. In other words the surface is strongly damaged. The morphological changes at different temperatures are shown by Fig. 2b at 308 K, Fig. 2d at 318 K, Fig. 2f at 328 K in presence of inhibitor at optimum concentration (100 mg/L). These images in presence of inhibitor are comparatively smooth and less corroded than in its absence. This result provides an evidence that inhibitor effectively protect the aluminum from corrosion.

### 3.2.2. AFM

The three-dimensional AFM images of aluminum surface without and with the presence of inhibitor are shown in Fig. 3(a,b). In uninhibited solution, aluminum surface was damaged strongly attributed to the dissolution of oxide film and average roughness reaches up to 80  $\mu\text{m}$  (Fig. 3a). When inhibitor at optimum concentration (100 mg/L) was added in that solution the surface appears more flat, homogeneous and uniform and average roughness decrease to 5.10  $\mu\text{m}$  (Fig. 3b). These results suggested that the inhibitor showed an appreciable resistance to corrosion.

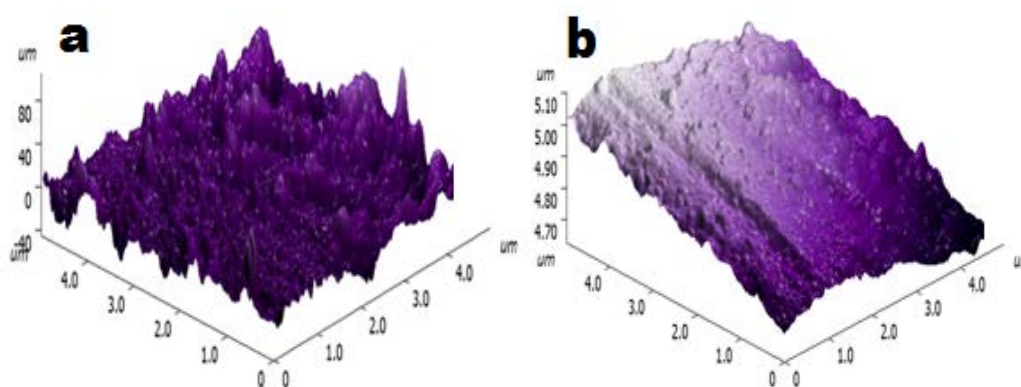


**Fig. 3.** AFM images (a) Blank (b) Inhibitor

## 3.3. Quantum chemical calculation

### 3.3.1. Neutral inhibitor

The optimized geometry, HOMO and LUMO structures and quantum chemical parameters of studied inhibitor are given in Fig. 4 (a-c) and Table 2 respectively.

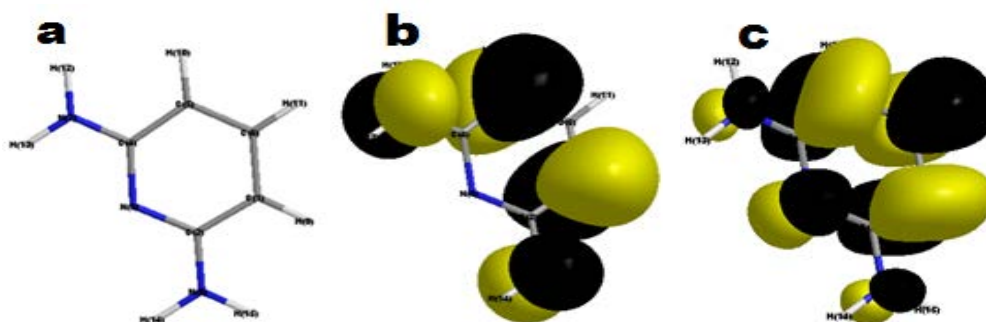


**Fig. 4.** (a) Optimized structure (Neutral) (b) HOMO (Neutral) (c) LUMO (Neutral)

The electron donating ability is given by HOMO i.e. higher the value of HOMO greater would be its donation ability. In opposite, electron accepting ability is given by LUMO i.e. lower the value of LUMO higher would be its electron accepting ability [23]. And the difference between HOMO and LUMO is known as energy gap ( $\Delta E$ ) i.e. lower  $\Delta E$  value; higher would be the inhibition efficiency.

**Table 2.** Quantum chemical parameters of neutral and protonated inhibitor

Quantum chemical parameters	Inhibitor (neutral) (eV)	Inhibitor (protonated) (eV)
$E_{\text{HOMO}}$ (eV)	-0.570	-10.267
$E_{\text{LUMO}}$ (eV)	3.364	0.700
$\Delta E$ (eV)	3.934	10.967

### 3.3.2. Protonated inhibitor

The inhibitor molecules in aqueous medium have a tendency to undergo protonation and this protonated form of the inhibitor can absorb over the aluminium surface. So, it becomes very important to compare the electronic properties of the neutral and protonated species. The site which has most negative value of Mulliken charge would undergo protonation and in the present case it is N<sub>8</sub>.

The optimized geometry, HOMO and LUMO structures of protonated species are given in Fig. 5(a-c).

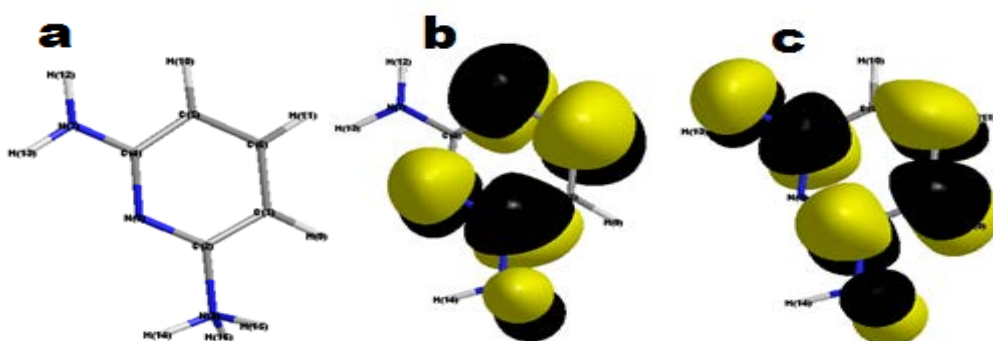


**Fig. 5.** (a) Optimized structure (protonated); (b) HOMO (protonated); (c) LUMO (protonated)

After comparing the quantum chemical parameters of neutral and protonated inhibitor (Table 2), we could conclude that neutral form of inhibitor has larger  $E_{\text{HOMO}}$  value as compared to its protonated form. This is an indication that neutral form of inhibitor has more tendencies to donate its electrons and, thereby, adsorb strongly over the aluminum surface. Also  $\Delta E$  in neutral form of inhibitor is lower than its protonated one, which is an indication that neutral one is more reactive than protonated one in the solution. Thus, the neutral form of inhibitor is more favorable to adsorb on the aluminum surface than protonated form.

#### 4. CONCLUSION

Tafel polarization confirmed that the inhibitor is mixed type but predominantly anodic and inhibition efficiency increases with increase in inhibitor concentration. SEM and AFM micrographs shows then protection of aluminum surface in presence of inhibitor. Quantum chemical study revealed that neutral form of inhibitor is more favorable to adsorb on the aluminum surface than protonated form.

#### Acknowledgement

K. R. Ansari gratefully acknowledges Ministry of Human Resource Development (MHRD), New Delhi, India for the financial assistance and facilitation of study.

#### REFERENCES

- [1] M. Dabala, E. Ramous, and M. Magrini, *Mater. Corros.* 55 (2004) 381.
- [2] P. Cavaliere, *Mater. Charact.* 57 (2006) 100.
- [3] R. Rosliza, W. B. Wan Nik, S. Izman, and Y. Prawoto, *Curr. Appl. Phys.* 10 (2010) 923.
- [4] J. A. Hill, T. Markley, M. Forsyth, P. C. Howlett, and B. R. W. Hinton, *J. Alloys Compd.* 509 (2011) 1683.
- [5] R. Rosliza, W. B. Wan Nik, and H. B. Senin, *Mater. Chem. Phys.* 107 (2008) 281.
- [6] M. J. Frisch et al., *Gaussian 03*, Revision E.01, Gaussian Inc., Wallingford CT (2007).
- [7] W. Villamizar, M. Casales, J. G. Gonzalez-Rodriguez, and L. Martinez, *J. Solid State Electrochem.* 11 (2007) 619.
- [8] W. Villamizar, M. Casales, L. Martinez, J. G. Chacon-Naca, and J. G. Gonzalez-Rodriguez, *J. Solid State Electrochem.* 12 (2008) 193.
- [9] K. R. Ansari, and M. A. Quraishi, *J. Assoc. Arab Univ. Basic Appl. Sci.* 18 (2015) 12.
- [10] K. R. Ansari, and M. A. Quraishi, *Physica E* 69 (2015) 322.
- [11] K. R. Ansari, M. A. Quraishi, and A. Singh, *Corros. Sci.* 79 (2014) 5.
- [12] K. R. Ansari, M. A. Quraishi, and A. Singh, *J. Ind. Eng. Chem.* 25 (2015) 89.

- [13] K. R. Ansari, Sudheer, A. Singh and M. A. Quraishi, *J. Dispersion Sci. Technol.* 36 (2015) 908.
- [14] K. R. Ansari, M. A. Quraishi, *Anal. Bioanal. Electrochem.* 7 (2015) 509.
- [15] S. Martinez, and M. M. Hucovic, *J. Appl. Electrochem.* 33 (2003) 1137.
- [16] M. A. Quraishi, K. R. Ansari, D. K. Yadav, and E. E. Ebenso, *Int. J. Electrochem. Sci.* 7 (2012) 12301.
- [17] K. R. Ansari, M. A. Quraishi, and A. Singh, *Measurement* 76 (2015) 136.
- [18] D. G. Ladha, P. M. Wadhvani, M. Y. Lone, P. C. Jha, and N. K. Shah, *Anal. Bioanal. Electrochem.* 7 (2015) 59.
- [19] A. Fattah-alhosseini, A. Moradi, E. Moradi, and N. Attarzadeh, *Anal. Bioanal. Electrochem.* 6 (2014) 284.
- [20] K. R. Ansari, and M. A. Quraishi, *J. Ind. Eng. Chem.* 20 (2014) 2819.
- [21] K. R. Ansari, and M. A. Quraishi, *J. Taiwan Inst. Chem. Eng.* 54 (2015) 145.
- [22] K. R. Ansari, M. A. Quraishi, and A. Singh, *Corrosion Sci.* 95 (2015) 62.
- [23] S. Zor, M. Saracoglu, F. Kandemirli, and T. Arslan. *Corrosion* 67 (2011) 1.